Available online at www.sciencedirect.com
ScienceDirect
Journal of Molecular Catalysis A: Chemical 278 (2007) 200–208
JOURNAL OF MOLECULAR CATALYSIS A: CHEMICAL
www.elsevier.com/locate/molcata

Gold nanoparticles: Support effects for the WGS reaction

Alberto Sandoval [a], Antonio Gómez-Cortés [b], Rodolfo Zanella [a,*], Gabriela Díaz [b,**], José M. Saniger [a]

[a] *Centro de Ciencias Aplicadas y Desarrollo Tecnológico, Universidad Nacional Autónoma de México (UNAM), Circuito Exterior S/N, A. P. 70-186, C. P. 04510, Ciudad Universitaria, México D.F., Mexico*
[b] *Instituto de Física, Universidad Nacional Autónoma de México (UNAM), Circuito de la Investigación Científica S/N, A. P. 20-364, C. P. 01000, México D.F., Mexico*

Received 7 June 2007; received in revised form 6 September 2007; accepted 9 September 2007
Available online 18 September 2007

Abstract

Gold nanoparticles supported on reducible (TiO_2 and CeO_2) and non-reducible oxides (Al_2O_3 and SiO_2) with comparable gold particle size (2.5–3.5 nm) were studied as catalysts in the WGS reaction. Deposition–precipitation with urea (DP Urea) was used to prepare gold nanoparticles supported on TiO_2, CeO_2 and Al_2O_3. Cationic adsorption was used as preparation method in the case of SiO_2. Metal loading was fixed to 4 and 8 wt.%. The WGS reaction was studied in the temperature range from 50 to 400 °C in a flow reactor at atmospheric pressure. Before reaction the samples were calcined at 200, 300 or 400 °C to study the effect of calcination temperature in the catalyst activity. The Au/CeO_2 catalyst showed an enhanced reduction at low-temperatures as evidenced by the H/Au ratio. The lowest reduction temperature was observed for gold in the Au/TiO_2 catalyst. When supported on TiO_2 and CeO_2, the activity of gold nanoparticles was much higher than the one observed when supported on Al_2O_3 and SiO_2 being the Au/SiO_2 catalyst practically inactive. For samples calcined at 300 °C and reaction temperatures below 225 °C the activity varied as follows: $TiO_2 > CeO_2 \gg Al_2O_3$. CO adsorption in the presence of H_2O was followed by DRIFT. Bands coming from C–H stretching associated to formate species were clearly observed on CeO_2. Intensity of these bands decreased when Au is present on the supports. Au^0-CO adsorption band was evidenced when Au is supported on TiO_2, CeO_2 and Al_2O_3. Fast conversion of formate species in Au/TiO_2 and Au/CeO_2 takes place and this explains the higher activity displayed by these catalysts.

Keywords: Gold; Water gas shift; Support reducibility; Catalysts pretreatment; CO adsorption

1. Introduction

The water gas shift (WGS) is a key reaction in the production of hydrogen for a number of processes, including petroleum refining and chemicals synthesis. An emerging application for the WGS is the production of hydrogen for proton exchange membrane (PEM) fuel cells. This reaction is important because it removes CO, a poison to the fuel cell electrocatalysts, which is produced during the steam reforming and/or partial oxidation reactions. Moreover, WGS reaction is one of the key steps involved in the automobile exhaust processes, converting CO and water to hydrogen and CO_2 and including the produced hydrogen as a very effective reductant for NO_x removal [1,2].

Copper- and Fe-Cr-based catalysts have been used commercially for the WGS; however, they are not suitable for portable and vehicular applications because of insufficient durability and activities. Consequently, there is substantial interest in the development of better performing and more durable WGS catalysts [3–5].

Presently great attention is paid to gold-containing catalysts because of their high catalytic activity at low-temperatures in a series of important reactions, such as oxidation of CO and H_2 [6], reduction of NO_x [7], epoxidation of C_3H_6 [8], selective CO oxidation in hydrogen rich stream [9] and combustion of methane [10]. In 1996 Andreeva et al. [11] reported that metallic gold nanoparticles on Fe_2O_3 prepared by coprecipitation showed good activity in the low-temperature WGS. In 1997 Sakurai et al. [12] reported that Au/TiO_2, prepared by

* Corresponding author. Tel.: +52 5556228602x1115; fax: +52 5556228651.
** Corresponding author. Tel.: +52 5556225097; fax: +52 5556225008.
E-mail addresses: rodolfo.zanella@ccadet.unam.mx (R. Zanella), diaz@fisica.unam.mx (G. Díaz).

1381-1169/$ – see front matter © 2007 Elsevier B.V. All rights reserved.
doi:10.1016/j.molcata.2007.09.014

deposition–precipitation, was active for the low-temperature WGS in a mixed gas of CO, H_2O and He. The Au/TiO_2 catalyst presented comparable WGS activity to that of commercial Cu/ZnO/Al_2O_3 catalysts [12].

The WGS reaction is thought to occur mainly through two reaction mechanisms, the regenerative, redox mechanism and the associative mechanism. According to the redox mechanism, the WGS reaction proceeds via consecutive steps of reduction and oxidation of the catalyst surface [3,5]. The redox mechanism is believed to occur mainly on high-temperature shift catalysts, where reducible supports are used. The associative mechanism involves interaction between CO molecule and surface intermediates (mainly formates), which further decompose to reaction products, CO_2 and H_2 [13–16]. Fu et al. [17] proposed that non-metallic gold species strongly associated with surface cerium-oxygen groups are responsible for activity. Conversely, other authors propose that probably a metallic function participates in the surface catalytic mechanism [15]. It is proposed that the WGS reaction proceeds at the boundary between small metallic particles and support [16].

There is a general consensus that the preparation method, the synthesis parameters, pretreatment conditions, the choice of the support and the Au particle size exert a significant influence on the ultimate catalytic performance of gold supported systems [18]. The Au particle size and structure are sensitive to a number of variables, including the preparation method [18–20] the state and structure of the support [18,21,4] and the catalyst pretreatment [22–25]. Gold catalysts differ from other noble metals catalysts in the crucial importance of the preparation method for the genesis of catalytic activity. The preferred technique for the preparation of highly dispersed Au-based catalysts is the deposition–precipitation method [19,26,16].

Related with the catalyst pretreatment, in the best of our knowledge, very few works related with the WGS reaction have studied systematically the effect of the calcination temperature on the catalytic activity of gold supported nanoparticles [27]. Hua et al. [27] have shown that catalysts calcined at 200 °C display the highest catalytic activity. However, several works related with gold nanoparticles supported on TiO_2 [12,28,29], TiO_2 nanotubes [30], CeO_2 [14,31,17,16], Fe_2O_3 [4,32], ZnO [4] and ZrO_2 [4] have used 400 °C as calcination temperature, but in most of cases it is not clearly justified why this temperature is chosen.

On the other side, the prerequisite for the synthesis of a highly active gold supported catalyst is not only to obtain a high dispersion of gold particles but also to choose an appropriate support for the reactions. The activity and specially the stability of the gold catalysts depend on both the state and structure of the support and the specific interaction between gold and the support. The support is considered crucial as a source of oxygen [18,33] or for otherwise stabilizing Au in the active nanostructured form [34].

The Au/support interface is a model of a metal-semiconductor or metal-insulator junction bearing unique size-dependent electronic properties, which could play an essential role in the origin of the catalytic activity. The supports, generally being metal oxides, are divided into two categories: the reducible (Fe_2O_3, TiO_2, Co_2O_3, CeO_2, ZrO_2) and the non-reducible supports (SiO_2, Al_2O_3, MgO) [33]. Previous studies indicated that gold particles finely dispersed (2–5 nm) on reducible supports such as Fe_2O_3, TiO_2, ZrO_2 exhibit high catalytic activity in the low-temperature WGS reaction [11,12,4]. Moreover recently, several groups have reported the low-temperature catalytic activity of Au/CeO_2 catalysts [35,5,31,14].

In this work, we perform a comparative study on the effect of the activation temperature and the nature of the support of gold supported catalysts for the WGS reaction. Comparison was made using reducible (TiO_2 and CeO_2) and non-reducible (Al_3O_3 and SiO_2) oxides in order to determine the role of the support on the catalytic activity of the gold particles.

2. Experimental

2.1. Catalyst preparation

TiO_2 (Degussa P25, 49 m^2/g), CeO_2 (Alfa-Aesar 76 m^2/g), Al_2O_3 (Degussa Aeroxide 101 m^2/g) and SiO_2 (Degussa Aerosil 200, 198 m^2/g) were used as supports. Commercial $HAuCl_4.3H_2O$ (Aldrich) and freshly prepared $[Au(en)_2]Cl_3$ were used as gold precursors. The $[Au(en)_2]^{3+}$ complex was prepared as described by Block and Bailar [36].

Catalysts were prepared in the absence of light, which is known to decompose and reduce gold precursors. Before preparation, oxides were dried in air at 100 °C for at least 24 h. Gold nanoparticles on TiO_2, CeO_2 and Al_2O_3 were obtained by deposition–precipitation with urea (DP Urea) following the previously reported procedure [19,20]. Au/SiO_2 samples preparation was done by cationic adsorption [37]. The SiO_2 support (1 g) was dispersed in 100 mL of an aqueous solution of $[Au(en)_2]Cl_3$ (4×10^{-3} M) previously heated at 45 °C. In order to promote the cationic adsorption of $[Au(en)_2]^{3+}$ complex on SiO_2, the pH of the solution was adjusted to a value of 10 which is higher than the IEP_{SiO_2} by dropwise addition of 1 M ethanediamine solution. The suspension was vigorously stirred for 2 h at 45 °C in a thermostated vessel. A similar method has been used to deposit gold nanoparticles on mesoporous silica (SBA-15) [38].

After deposition of gold onto the support, the solids were separated from the precursor solution by centrifugation (5000 rpm for 12 min), washed with 100 mL of distilled water under stirring for 10 min at 40 °C, and then centrifuged. The operation was repeated several times. The solids were dried under vacuum at 100 °C for 2 h in the case of DP Urea preparations and under vacuum at room temperature for 24 h in the case of cationic adsorption preparations. The dried samples were stored in the dark under vacuum in a desiccator. Nominal Au loading was 4–8 wt.%. Samples will be identified as follows: XAu/MO where X is the nominal Au loading and MO is the TiO_2, CeO_2, Al_2O_3 or SiO_2 supports.

Before any characterization the samples were calcined at 200, 300 or 400 °C under air flow (100 mL min^{-1}, Praxair) at a heating rate of 2 °C min^{-1} and maintained 6 h at the chosen temperature.

2.2. Characterization techniques

Thermally treated samples were examined by high resolution transmission electron microscopy (HRTEM) in a 2010 FasTem analytical microscope equipped with a Z-contrast annular detector. About 500 particles were measured to get information about the average particle size and size distribution.The average particle size d_{av} was calculated from the following formula: $d_{av} = \sum n_i d_i / \sum n_i$ where n_i is the number of particles of diameter d_i.

Chemical analysis of Au in the samples to determine the actual loading was performed by energy dispersive X-ray spectroscopy (EDS) with an Oxford-ISIS detector coupled to a scanning electron microscope (JEOL JSM-5900-LV). Chemical analysis was performed after thermal treatment of the samples. The Au weight loading is expressed in gram of Au per gram of sample, wt.% $Au = [m_{Au}/(m_{Au} + m_{MO})] \times 100$.

Hydrogen temperature programmed reduction (H_2-TPR) experiments were performed in a RIG-100 unit under a flow of 5% H_2/Ar gas mixture (30 mL min^{-1}) and a heating rate of 10 °C/min from room temperature to 800 °C. The H_2O produced by the reduction process was trapped before the TCD. Bulk CuO was used as reference for calibration of the TCD signal.

The CO + H_2O reaction was followed by FTIR spectroscopy in a Nicolet Nexus 470 spectrophotometer using an environmentally controlled high-pressure/high-temperature Spectra Tech DRIFT cell with ZnSe windows. For each experiment 0.025 g of the dried sample was packed directly in the sample holder and pretreated in situ under air flow (30 mL min^{-1}) at 300 °C for 1 h. After this treatment the sample was purged with He at 300 °C and then cooled to room temperature in the same gas atmosphere before admittance of 2.5% CO/He for 15 min. Afterwards, 0.65% vapor H_2O in He stream was introduced in the DRIFT cell. The total flow was 60 mL min^{-1}. Spectra were collected under reactant flow in the range RT-300 °C from 128 scans with a resolution of 4 cm^{-1}.

2.3. Catalytic activity

The WGS reaction was studied in the temperature range of 50–400 °C in a flow reactor at atmospheric pressure. Typically, 0.1 g of catalyst was calcined in air flow for 6 h at different temperatures (200–400 °C) before the catalytic run. Prior to the catalytic run the catalyst was purged in He before admittance of the reactant gas mixture which composition was 5% CO in He saturated with H_2O vapor (10%). The space velocity was 9000 h^{-1}. At each temperature, reaction was allowed to stabilize before collecting any data. The exit gases were analyzed by online GC (TCD) using a Carboxen 1000 packed column.

3. Results and discussion

3.1. TPR characterization

The reduction properties of the catalysts were studied by TPR. Fig. 1 displays the TPR profiles of 4Au/MO samples, which are in general characterized by a more or less broad reduction peak, with a maximum which depends on the support. In

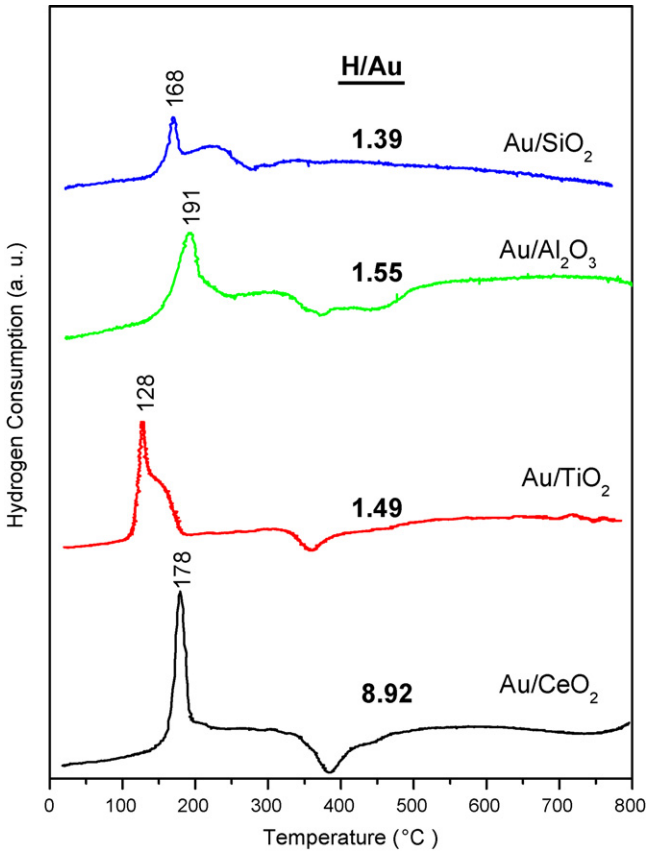

Fig. 1. TPR profiles of Au supported catalysts. Hydrogen consumption presented as the H/Au experimental ratio corresponds to peaks below 350 °C.

the case of Au/SiO_2, T_{max} is 168 °C, this peak must be related with the Au^{3+} reduction. A second, more or least, broad peak is observed at T_{max} = 222 °C and has been related with the Au^{1+} to Au^0 reduction or with the reduction of small ionic gold grains encapsulated in partly reduced Au clusters [39]. For Au/Al_2O_3 a peak with a maximum at 191 °C is observed. Gluhoi et al. [39] on Au/Al_2O_3 samples reported a similar peak at 163 °C which was related to the reduction process $Au^{3+} \rightarrow Au^0$. Differences between experimental protocols such as heating ramp, flow rate or concentration of the reducing gas may explain the difference in the position of T_{max} between the reported results and ours.

In the case of Au/TiO_2, the reduction profile is characterized by a peak with a maximum at T = 128 °C. A low-temperature reduction peak like this has already been observed for Au/TiO_2 samples [40,41], and assigned to the reduction of oxygen species on the nanosized gold particles and eventually to the $Ti^{4+} \rightarrow Ti^{3+}$ reduction of sites at the interface with gold particles [42,41,29].

For ceria containing samples, two reduction peaks have been reported in TPR profiles of pure ceria support. A low-temperature peak at about 500 °C, has been assigned to the reduction of surface oxygen species and a high-temperature peak (>800 °C), was assigned to the reduction of bulk oxygen and to the formation of lower oxides of cerium. Also it was observed that the first peak could be significantly shifted to lower temperatures in the presence of gold [35]. In the case of Au/CeO_2 samples, the peaks assigned to ceria surface layer reduction have been located within the temperature range 120–160 °C [43]. In

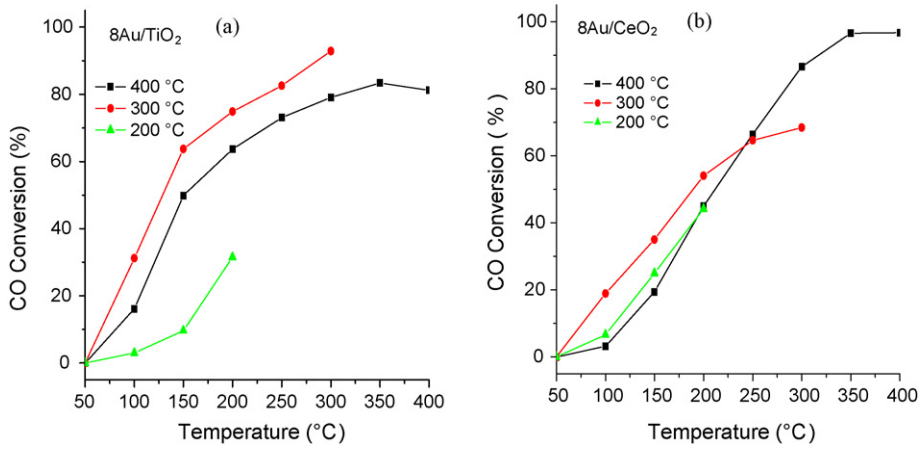

Fig. 2. CO conversion vs. reaction temperature in the WGS using (a) $8Au/TiO_2$ and (b) $8Au/CeO_2$ catalysts activated at 200, 300 and 400 °C.

our Au/CeO_2 sample a peak is observed at 178 °C. Andreeva et al. [35] have proposed that TPR peaks in this temperature range is the result of two overlapping peaks, one of which could be connected with the reduction of the oxygen species on the fine gold particles and the second one with the surface ceria reduction. Quantitative measurements of the H_2 consumption during the TPR experiments, characterized by the experimental H/Au ratio (Fig. 1), showed for Au/TiO_2, Au/Al_2O_3 and Au/SiO_2 samples, values in the range 1.4–1.6 which is close to the stoichiometric value expected for the Au^{3+} reduction process taking into account the actual gold loading as determined by EDS analysis. In the case of Au/CeO_2 catalyst (Fig. 1), an enhanced reduc-

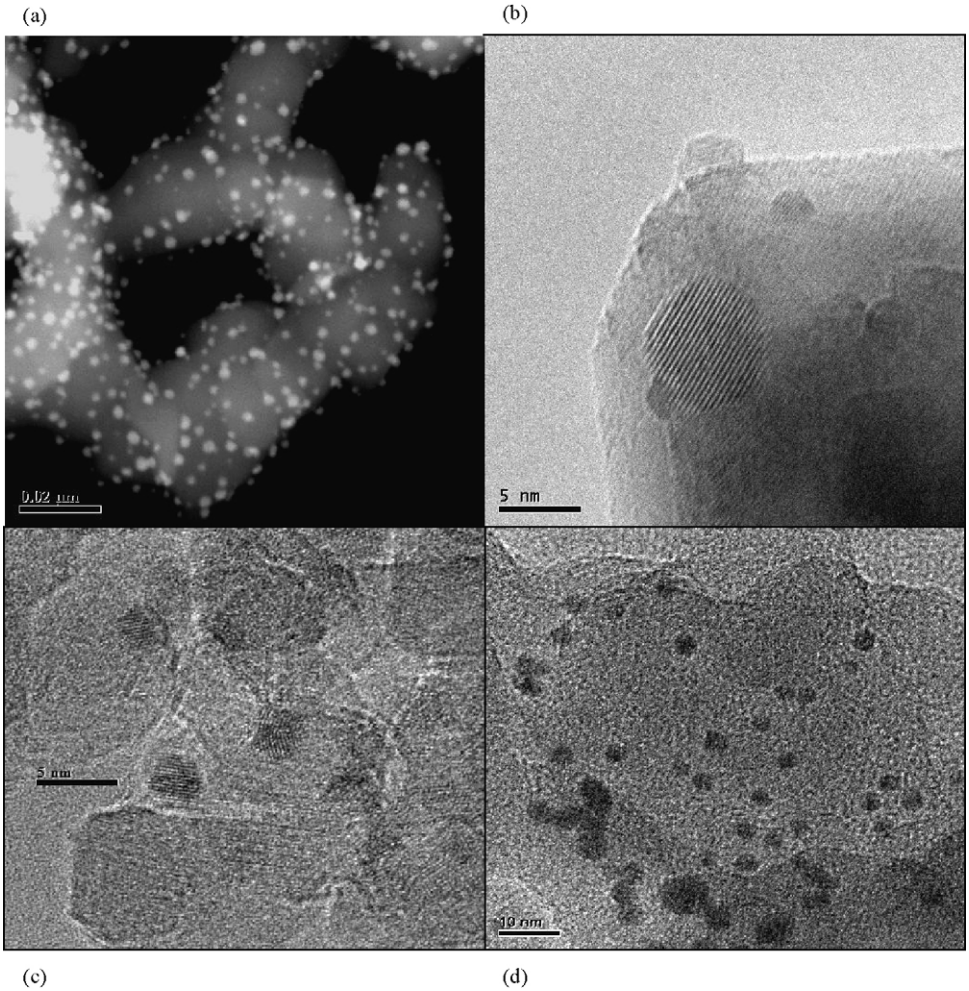

Fig. 3. HRTEM characterization of gold supported catalysts calcined at 300 °C. (a) Z-contrast image of $8Au/TiO_2$, (b) HRTEM image of $4Au/CeO_2$, (c) $8Au/Al_2O_3$ and (d) $8Au/SiO_2$.

tion at low-temperatures is observed as confirmed by the very high value (8.92) of the H/Au ratio. This result supports the assumption that the low-temperature reduction peak observed in Au/CeO_2 catalysts is related with both the reduction of Au^{3+} species and the reduction of surface ceria species. The presence of gold actually promotes a surface support reduction at temperatures lower than 300 °C.

The fact that the H_2 consumption of Au/TiO_2 sample is almost the same of gold supported on essentially non-reducible supports such as Al_2O_3 and SiO_2 make us believe that the observed reduction process is only related with the Au^{3+} species reduction and not with the reduction of the support.

3.2. Effect of pretreatment temperature on WGS activity

The effect of thermal treatment at different temperatures on the activity of the catalysts measured as the CO conversion in the WGS is presented in Fig. 2 for Au supported on TiO_2 and CeO_2. Samples were calcined at temperatures between 200 and 400 °C. These thermal treatments lead to the decomposition of Au(III) complexes into gold metal particles [23]. It must be remembered that the thermal treatment used to reduce Au^{III} into Au^0 can be performed with any gas (reducing gases such as H_2, or oxidizing gases such as air). When the supported gold precursor thermally decomposes in air, it forms Au^0 because of the instability of Au^{3+} species ($\Delta H_f(Au_2O_3) = 19.3\ kJ\ mol^{-1}$) [44]. As observed in Fig. 2, calcination at 300 °C produced the most active sample in both cases, although, the effect of calcination temperature seems to be different in Au/CeO_2. In this catalyst, at low reaction temperature ($T_R < 200$ °C) the activity displayed by samples calcined at 200 and 400 °C is practically the same while for Au/TiO_2 clear differences are observed. Also, at high reaction temperatures ($T_R > 250$ °C) Au/CeO_2 catalyst calcined at 400 °C is significantly more active than the one activated at 300 °C. The bare CeO_2 support transforms around 6% CO at 250 °C.

The results obtained here about the influence of calcination temperature on the catalytic behavior of Au/TiO_2 and Au/CeO_2 differ from previously reported on Au/Fe_2O_3 catalysts [27]. In that work was shown that catalysts calcined at 200 °C showed rather high catalytic activity than catalysts calcined at 300, 350, 450 and 550 °C. Based on results for gold supported catalysts from which most of the Au was leached, it was claimed that ionic Au was primarily responsible for the high WGS activity [17]. Conversely, Tabakova et al. [16] proposed that the reaction proceeds at the boundary between nanosized metallic particles and ceria, where CO adsorption on small gold metallic nanoparticles and H_2O dissociation on oxygen-vacancy defects of ceria take place. Moreover, it has been proposed that the WGS feed, through surface reduction, activates the catalyst, since the reduction occurs at very low-temperature [14]. XANES results of Au/CeO_2 [45] have showed that Au is in its reduced form when it promotes the surface shell reduction of ceria [14]. Our own Au/TiO_2 XANES and EXAFS results of samples prepared by DP Urea method shown that all the gold is in metallic form at calcination temperatures superior or equal to 200 °C [23]. These reported results as well as our TPR results do not support the proposal that active non-metallic species are responsible for WGS activity.

3.3. TEM characterization and effect of gold loading

HRTEM examination of samples calcined at 300 °C showed an initial average gold particle size for all the supports of ca. 2.5–3.5 nm. A unimodal particle size distribution was practically obtained and only the $8Au/TiO_2$ and $8Au/CeO_2$ catalysts presented a slight tendency to a bimodal distribution. On the other hand, XRD patterns of all samples did not revealed peaks related to gold, confirming that the gold was deposited as small particles. In Fig. 3 some typical images of HRTEM and Z-contrast of Au/MO samples are shown.

The effect of Au loading (4 and 8 wt.%) for samples calcined at 300 °C was also examined. Fig. 4 presents the WGS rate as a function of reaction temperature for Au supported on TiO_2 and CeO_2. As observed in both cases, low loading samples ($4Au/TiO_2$ and $4Au/CeO_2$) are more active. This result may be understood taking into account that at high Au loading sintering of gold particles may take place leading to a diminution of

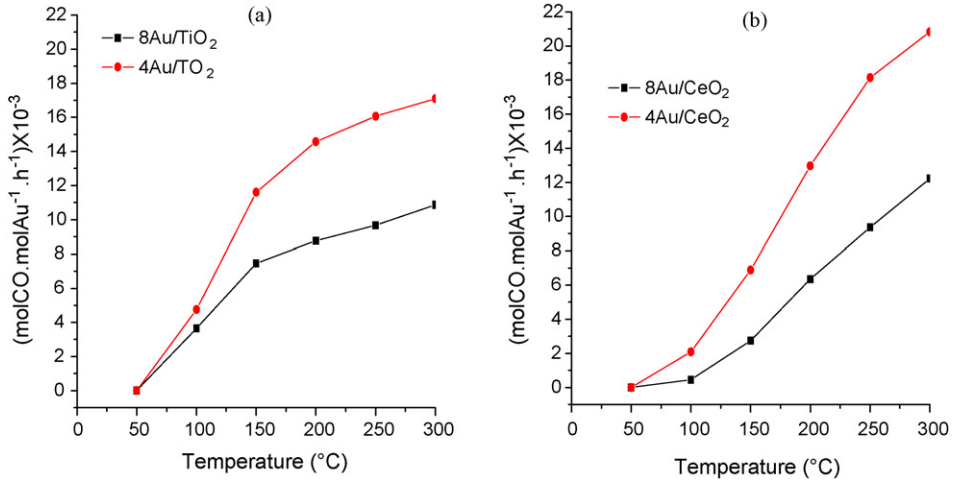

Fig. 4. Effect of Au loading for catalysts calcined at 300 °C. Activity of Au/TiO_2 and Au/CeO_2 catalysts.

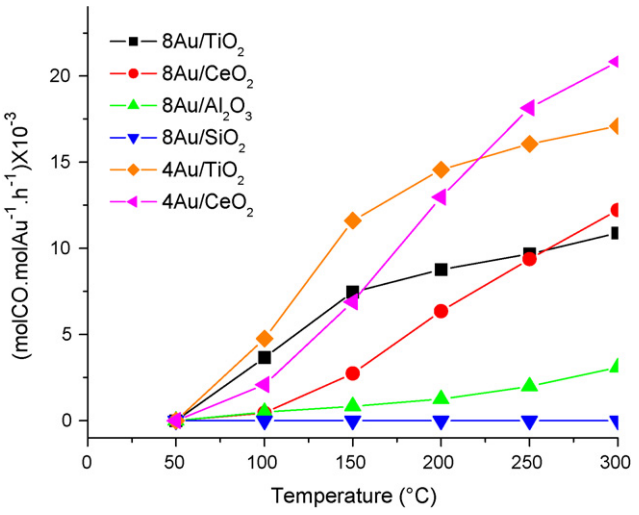

Fig. 5. Catalytic activity in the WGS as a function of reaction temperature displayed by Au nanoparticles supported on TiO_2, CeO_2, Al_2O_3 and SiO_2.

active sites for the reaction. Since average particle size is about the same, this would be in line with the observation of a bimodal size distribution in high loading catalysts. These results are in agreement with the previously reported by Idakiev et al. [30] who showed that for Au/TiO_2 samples with lower gold loading exhibits higher CO conversion than the sample with higher gold content. The higher activity of the sample with lower gold loading was related to the size of Au particles and to the contact structure of Au nanoparticles with the support.

3.4. Effect of the support on WGS activity

In view of the catalytic behavior of the samples as a function of the activation temperature, the catalytic performance for the WGS reaction was compared for catalysts activated at 300 °C. Fig. 5 displays the WGS rate in terms of the actual gold loading. The activity of gold nanoparticles on the reducible supports (TiO_2 and CeO_2) was much higher than the one observed when supported on Al_2O_3 and SiO_2 being the Au/SiO_2 catalyst practically inactive. It must be noted that recently it has been reported that Au/SiO_2 catalysts prepared by cation adsorption were very active for CO oxidation below 0 °C [46]. Noble metals (Pt, Rh, Ru, and Pd) on irreducible supports as SiO_2 are 1–2 orders of magnitude less active in the WGS compared to catalysts supported on TiO_2 and CeO_2 [47]. For reaction temperatures below 225 °C the activity varied as follows: $TiO_2 > CeO_2 \gg Al_2O_3$. At reaction temperatures above 225 °C, the $4Au/CeO_2$ catalyst is more active compared to the $4Au/TiO_2$ one.

3.5. FTIR characterization

Infrared spectroscopy of adsorbed CO and after admission of H_2O was used to get more information about the reactive

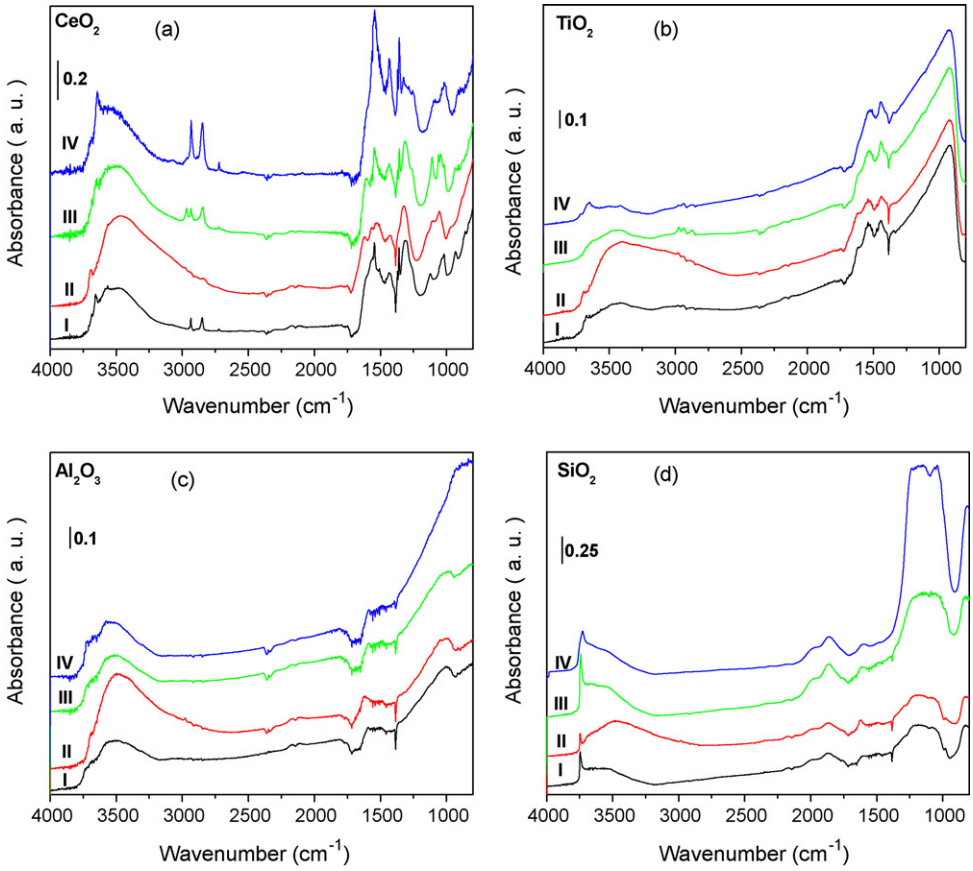

Fig. 6. DRIFT spectra collected under CO flow and after admission of H_2O at various reaction temperatures on (a) CeO_2, (b) TiO_2, (c) Al_2O_3 and (d) SiO_2 supports. Spectra I, II, III and IV correspond, respectively, to CO adsorption at RT, CO + H_2O at RT, CO + H_2O at 150 °C and CO + H_2O at 300 °C.

surface in the catalysts. Spectra were taken from supports and fresh catalysts calcined in situ at 300 °C after adsorption of CO at RT followed by admission of H_2O in the DRIFT cell. Spectra of CO + H_2O mixtures were collected after heating the cell from room temperature to 300 °C. The interaction of CO with the support hydroxyl groups yields formate species which are characterized by absorption bands in the following spectral regions 1340–1400 cm^{-1} (ν_s COO), 1550–1620 cm^{-1} (ν_{as} COO) and 2700–2900 cm^{-1} (ν_{C-H}) [48]. Absorption bands from formate species due to C–H stretching vibrations were clearly observed in the case of CeO_2 support (Fig. 6a, spectra I). On the other hand, absorption bands at 1000–1700 cm^{-1} characterize adsorbed carbonate-carboxylate species [48]. A complex structure in this region was observed in the case of CeO_2 (Fig. 6a, spectra I) where monodentate and bidentate carbonate species could be identified. The bands at 1622, 1432 and 1225 cm^{-1} are characteristic of the stretching vibrations of bicarbonate species [49–51]. After H_2O is admitted in the cell at RT (spectra II), the band in the 3600–2500 cm^{-1} region associated to the OH stretching modes of adsorbed water molecules increases in all samples and the C–H stretching bands, mostly those at 2930, 2847 and 2721 cm^{-1}, become important in the case of CeO_2 at high-temperature (Fig. 6a, spectra III and IV) and those at 2976, 2930 and 2868 cm^{-1} at 150 °C (Fig. 6b, spectra III). In the carbonate region, the structure of the bands remains complex with a clear increase in the intensity of the band at 1545 cm^{-1} at 300 °C in the case of ceria.

To study the interaction of CO in absence and presence of H_2O on supported gold catalysts, the 4Au/MO samples were used. After CO adsorption at RT a strong band at ca. 2108 cm^{-1} is present in TiO_2, CeO_2, and Al_2O_3 catalysts (Fig. 7a–c, spectra I). This band has been assigned to CO chemisorption on gold metallic particles [52,53]. The Au^0-CO band is still observed after admission of H_2O at RT in the cell in the case of Au/TiO_2 and Au/Al_2O_3 (Fig. 7b and c, spectra II) while for Au/CeO_2 has almost disappeared (Fig. 7a, spectra II). A strong increase in intensity of the absorption in the 3600–2500 cm^{-1} region due to the OH stretching of adsorbed water is observed in all cases (Fig. 7, spectra II). As temperature increases the intensity of the Au^0-CO band decreases and changes in the structure of the carbonate region are observed mostly in the Au/CeO_2 and Au/Al_2O_3 samples. In the presence of gold, the intensity of the formate bands observed on the bare ceria and titania supports dramatically decreased (Fig. 7a and b). Fast conversion of formate species in Au/TiO_2 and Au/CeO_2 takes place and this explains the higher activity displayed by these catalysts.

In the case of Au/SiO_2 (Fig. 7d) no Au^0-CO band was observed in the carbonyl region suggesting either that Au^{3+} has not been fully reduced in this catalyst or that gold particles were not accessible to CO. As the catalyst was thermally treated at

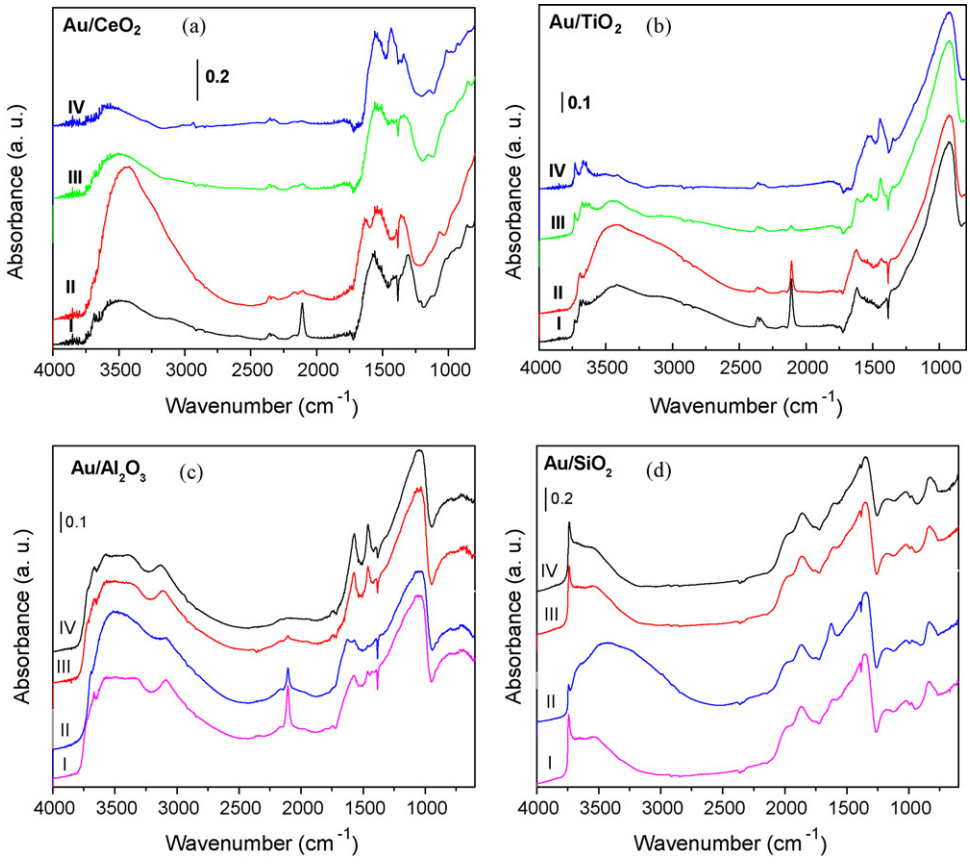

Fig. 7. DRIFT spectra collected under CO flow and after admission of H_2O at various reaction temperatures for (a) $4Au/CeO_2$, (b) $4Au/TiO_2$, (c) $4Au/Al_2O_3$ and (d) $4Au/SiO_2$ catalysts. Spectra I, II, III and IV correspond, respectively, to CO adsorption at RT, CO + H_2O at RT, CO + H_2O at 150 °C and CO + H_2O at 300 °C.

300 °C to reduce Au^{3+} which occurs as evidenced by the H/Au ratio in the TPR experiments and confirmed by the absence of CO bands of CO adsorbed on cationic gold sites (2150–2180 cm^{-1}, region) in the DRIFT spectra, the first suggestion seems not adequate. TPO experiments (not shown) performed on Au/SiO_2 catalysts prepared using the $[Au(en)_2]^{3+}$complex showed that evolution of carbon as $CO–CO_2$ occurred at temperatures higher than 450 °C. It seems possible that carbon residues from the gold complex used to prepare the catalyst could be blocking the surface of gold particles and making it inaccessible to CO. In any case, even if gold nanoparticles in this catalyst are tailored in nanometer size, reducibility of the oxide support plays a crucial role on the catalytic performance of dispersed noble metal catalysts. This property may either have a direct or indirect effect on activity, as evidenced by the reaction mechanisms [3,5,13–16] proposed for this reaction.

4. Conclusions

The behavior of gold supported on reducible (TiO_2 and CeO_2) and non-reducible (SiO_2 and Al_2O_3) oxides was studied in the water gas shift reaction. The samples were prepared by liquid phase methods (DP Urea or cationic adsorption). In all cases small gold particles (2.5–3.5 nm) were obtained. TPR experiments for Au/TiO_2, Au/Al_2O_3 and Au/SiO_2 samples, showed experimental H/Au ratio very close to the stoichiometric value expected for the Au^{3+} reduction process. An enhanced reduction evidenced by the high H/Au ratio was observed for Au/CeO_2 sample, and related with both the reduction of Au^{3+} species and the reduction of surface ceria species. The Au/TiO_2 presented the lowest reduction temperature.

Reduction of Au precursors by calcination in air at 300 °C produced the most active samples for the WGS reaction. The activity of Au on TiO_2 and CeO_2 was much higher than the one observed when supported on Al_2O_3 being the Au/SiO_2 catalyst practically inactive. For reaction temperatures below 225 °C the activity varied as follows: $TiO_2 > CeO_2 \gg Al_2O_3$. At reaction temperatures above 225 °C, the Au/CeO_2 catalyst is more active compared to the Au/TiO_2 one. DRIFT experiments under reaction conditions after activation in situ of the samples (calcination in air at 300 °C) showed absorption bands related to stable formate species which are present mostly on the bare CeO_2 support. Intensity of these bands decreases when Au is present on the support. Au^0-CO adsorption band is evidenced when Au is supported on TiO_2, CeO_2 and Al_2O_3. Also, a complex band structure in the carbonate region was observed for Au/CeO_2. Fast conversion of formate species in Au/TiO_2 and Au/CeO_2 takes place which could be related with the higher activity displayed by these catalysts. In the case of Au/SiO_2, gold particles may not be accessible to CO probably due to the presence of carbon residues from the complex used in the catalyst preparation, but since the support has an important participation in the WGS reaction, the non-reducible nature of the silica support must also be taken into account to explain the poor catalytic behavior of this catalyst. The results presented here do not support the proposal that active non-metallic species are responsible for WGS activity.

Acknowledgements

Technical help from Luis Rendón LCM-IF (HREM) and Ivan Puente USAI-FQ (EDS) is acknowledged. R. Zanella and J.M. Saniger are indebted to UNAM Nanoscience and Nanotechnology project (PUNTA), DGAPA IN106507 and CONACYT 55154 grants for financial support. G. Díaz acknowledges DGAPA IN-117706 and CONACYT 42666-F projects which infrastructure was used in this work.

References

[1] M.M. Mohamed, T.M. Salama, M. Ichikawa, J. Col. Interf. Sci. 224 (2000) 366–371.
[2] I.B. Whittington, J.C. Jiang, L.D. Trimm, Catal. Today 26 (1995) 41–44.
[3] T. Bunluesin, R.J. Gorte, G.W. Graham, Appl. Catal. B 15 (1998) 107–114.
[4] T. Tabakova, V. Idakiev, D. Andreeva, I. Mitov, Appl. Catal. A 202 (2000) 91–97.
[5] Q. Fu, A. Weber, M. Flytzani-Stephanopoulos, Catal. Lett. 77 (2001) 87–95.
[6] M. Haruta, N. Yamada, T. Kobayashi, S. Iijima, J. Catal. 115 (1989) 301–309.
[7] A. Ueda, M. Haruta, Gold Bull. 32 (1999) 3–11.
[8] B.S. Uphade, Y. Yamada, T. Akita, T. Nakamura, M. Haruta, Appl. Catal. A 215 (2001) 137–148.
[9] G.K. Bethke, H.H. Kung, Appl. Catal. A 194–195 (2000) 43–53.
[10] R.J.H. Grisel, P.J. Kooyman, B.E. Nieuwenhuys, J. Catal. 191 (2000) 430–437.
[11] D. Andreeva, V. Idakiev, T. Tabakova, A. Andreev, R. Giovanoli, Appl. Catal. A 134 (1996) 275–283.
[12] H. Sakurai, A. Ueda, T. Kobayashi, M. Haruta, Chem. Commun. (1997) 271–272.
[13] T. Shido, Y. Iwasawa, J. Catal. 136 (1992) 493–503.
[14] G. Jacobs, S. Ricote, P.M. Patterson, U.M. Graham, A. Dozier, S. Khalid, E. Rhodus, B.H. Davis, Appl. Catal. A 292 (2005) 229–243.
[15] G. Jacobs, S. Ricote, U.M. Graham, P.M. Patterson, B.H. Davis, Catal. Today 106 (2005) 259–264.
[16] T. Tabakova, F. Boccuzzi, M. Manzoli, J.W. Sobczak, V. Idakiev, D. Andreeva, Appl. Catal. A 298 (2006) 127–143.
[17] Q. Fu, H. Saltsburg, M. Flytzani-Stephanopoulos, Science 301 (2003) 935–938.
[18] M. Haruta, Cattech 6 (2002) 102–115.
[19] R. Zanella, S. Giorgio, C.R. Henry, C. Louis, J. Phys. Chem. B 106 (2002) 7634–7642.
[20] R. Zanella, L. Delannoy, C. Louis, Appl. Catal. A 291 (2005) 62–72.
[21] M.M. Schubert, V. Plzak, J. Garche, R.J. Behm, Catal. Today 76 (2001) 143–150.
[22] S.D. Lin, M. Bollinger, M.A. Vannice, Catal. Lett. 17 (1993) 245–262.
[23] R. Zanella, S. Giorgio, C.H. Shin, C.R. Henry, C. Louis, J. Catal. 222 (2004) 357–367.
[24] R. Zanella, C. Louis, Catal. Today 107–108 (2005) 768–777.
[25] R. Zanella, C. Louis, S. Giorgio, R. Touroude, J. Catal. 223 (2004) 328–339.
[26] M. Haruta, S. Tsubota, T. Kobayashi, H. Kageyama, M.J. Genet, B. Delmon, J. Catal. 144 (1993) 175–192.
[27] J. Hua, K. Wei, Q. Zheng, X. Lin, Appl. Catal. A 259 (2004) 121–130.
[28] F. Boccuzzi, A. Chiorino, M. Manzoli, D. Andreeva, T. Tabakova, L. Ilieva, V. Iadakiev, Catal. Today 75 (2002) 169–175.
[29] V. Idakiev, T. Tabakova, Z.-Y. Yuan, B.L. Su, Appl. Catal. A 270 (2004) 135–141.
[30] V. Idakiev, Z.Y. Yuan, T. Tabakova, B.L. Su, Appl. Catal. A 82 (2005) 149–155.
[31] H. Sakurai, T. Akita, S. Tsubota, M. Kiuchi, M. Haruta, Appl. Catal. A 291 (2005) 179–187.
[32] D. Andreeva, T. Tabakova, V. Idakiev, Appl. Catal. A 169 (1998) 9–14.
[33] M.M. Schubert, S. Hackenberg, A.C.V. Veen, M. Muhler, V. Plzak, R.J. Behm, J. Catal. 197 (2001) 113–122.

[34] A.I. Kozlov, A.P. Kozlova, H. Liu, Y. Iwasawa, Appl. Catal. A 182 (1999) 9–28.
[35] D. Andreeva, V. Idakiev, T. Tabakova, L. Ilieva, P. Falaras, A. Bourlinos, A. Travlos, Catal. Today 72 (2002) 51–57.
[36] B.P. Block, J.C. Bailar Jr., J. Am. Chem. Soc. 73 (1951) 4722–4725.
[37] R. Zanella, A. Sandoval, P. Santiago, V.A. Basiuk, J.M. Saniger, J. Phys. Chem. B 110 (2006) 8559–8565.
[38] H. Zhu, C. Liang, W. Yan, S.H. Overbury, S. Dai, J. Phys. Chem. B 110 (2006) 10842–10848.
[39] A.C. Gluhoi, Z.X. Tang, P. Marginean, B.E. Nieuwenhuys, Top. Catal. 39 (2006) 101–110.
[40] D. Andreeva, T. Tabakova, L. Ilieva, A. Naydenov, D. Mehanjiev, M.V. Abrashev, Appl. Catal. A 209 (2001) 291–300.
[41] V. Idakiev, L. Ilieva, D. Andreeva, J.L. Blin, L. Gigot, B.L. Su, Appl. Catal. A 243 (2003) 25–39.
[42] J. Sobczak, D. Andreeva, Stud. Surf. Sci. Catal. 130 (2000) 3303–3308.
[43] L. Ilieva, G. Pantaleo, I. Ivanov, A.M. Venezia, D. Andreeva, Appl. Catal. B 65 (2006) 101–109.
[44] G.C. Bond, Gold Bull. 34 (2001) 117–119.
[45] G. Jacobs, U.M. Graham, E. Chenu, P.M. Patterson, B.H. Davis, J. Catal. 229 (2005) 499–512.
[46] H. Zhu, Z. Ma, J. Clark, Z. Pan, S.H. Overbury, S. Dai, Appl. Catal. A 326 (2007) 89–99.
[47] P. Panagiotopoulou, D.I. Kondarides, Catal. Today 112 (2006) 49–54.
[48] A.A. Davydov, in: C.H. Rochester (Ed.), Infrared Spectroscopy of Adsorbed Species on the Surface of Transition Metal Oxides, John Wiley & Sons, 1984.
[49] B. Aeijelts, A. Silberova, G. Mul, M. Makkee, J.A. Moulijn, J. Catal. 243 (2006) 171–182.
[50] F. Boccuzzi, A. Chiorino, M. Manzoli, D. Andreeva, T. Tabakova, J. Catal. 188 (1999) 176–185.
[51] N.M. Gupta, A.K. Tripathi, Gold Bull. 34 (2001) 120–128.
[52] F. Boccuzzi, A. Chiorino, S. Tsubota, M. Haruta, J. Phys. Chem. 100 (1996) 3625–3631.
[53] C. Ruggiero, P. Hollins, Surf. Sci. 377–379 (1997) 583–586.